15 Lectures on Tensor Numerical Methods for Multi-dimensional PDEs

Lect. 13-14. Integrating exotic oscillators. Solving equations with oscillating coefficients. IGA in tensor formats. Range-separated (RS) tensor format in many-particle modeling.

Boris Khoromskij, Venera Khoromskaia
Shanghai Jiao Tong University, April 2017

Max-Planck-Institute for Mathematics in the Sciences, Leipzig
MAX-PLANCK-GESELLSCHAFT

Lect. 13-14. Range-separated (RS) tensor format in many-particle modeling. Intergating exhotic oscillators. Equations with highly oscillating coefficients in log-complexity: alternative and generalization of geometric homogenization. IGA in tensor formats.

Outline of Lecture 13-14.

1. Fast QTT integration of exotic oscillators.
2. Discretization of PDEs with oscillating coefficients on fine spacial grid.
3. Preconditioning by homogenization scheme.
4. Preconditioned iteration in the QTT format: fast and robust in ε.
5. Discussion of numerics. Illustrations for the logarithmic complexity.
6. Tensor methods in Iso-Geometric Analysis (IGA)
7. Novel range separated (RS) tensor format and its applications.
8. Modern tensor numerical methods: main ingredients and challenging problems.

QTT based quadratures in 1D and 2D combined with QTT-cross approximation

(1D) Left: $f = C_1 sign(x) + C_2 + \sin(\omega x)$, $\omega = 20$. Grid size $N = 2^{22}$, QTT-rank $= 3$.

(1D) Middle: Sharp Gaussian $\exp(-\lambda x^2)$. Grid size $N = 2^{22}$, $\lambda = 100$,
$\varepsilon = 10^{-5}$ (3.2), 10^{-6} (3.5), 10^{-7} (3.7).

(2D) Right: 2D version of (A-1D). $f = 5 sign(x) + 6 + \sin(\omega x + \omega y)$,
$N \times N$ grid: $N = 2^9, 2^{10}$, $\varepsilon = 10^{-5}, 10^{-6}, 10^{-7}$, QTT-rank ≈ 3.5.

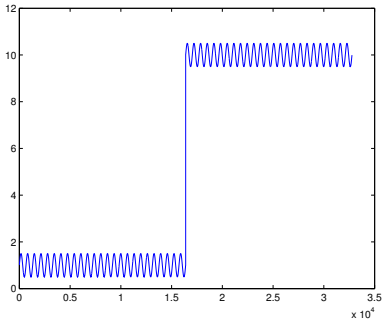
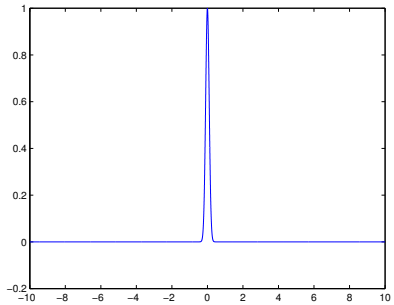
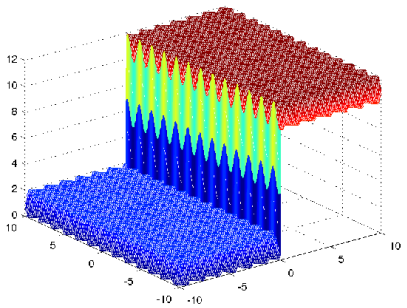

QTT-cross approximation by $O(r^2 \log N)$ samples.

Numerics confirms the theoretical QTT-rank estimates.

Twofold-QTT: fast quadratures for highly oscillating integrals + QTT in ω

Compute functions of $\omega \in [\omega_{min}, \omega_{max}]$, and for various $f(x), g(x)$, [BNK, Veit '14],

$$I_{\mathcal{R}e}(\omega, f) := \int_\Omega f(x)\cos(\omega g(x))dx, \quad I_{\mathcal{I}m}(\omega, f) := \int_\Omega f(x)\sin(\omega g(x))dx,$$

Example. Exotic oscillators which are not of the form $h_\omega(x) = e^{i\,\omega g(x)}$:

- Levin-type methods for the case of the Bessel oscillator $h_\omega(x) = J_\nu(\omega x)$, [Xiang, '08].
- Filon-type methods for oscillators of the form $h_\omega(x) = v(\sin(\omega\theta(x)))$, [Iserles, Levin, '11].
- For most other types of exotic oscillators such methods are not available so far.

- Our approach: Low rank QTT (cross) approx. of huge N-vectors for a function of ω,

$$I_{h_\omega,k}(\omega) := \int_{-1}^{1} T_k(x)h_\omega(x)dx, \quad \omega \in [\omega_{min}, \omega_{max}], \quad 1 \le k \le M$$

N	$[\omega_{\min}, \omega_{\max}]/h_\omega(x)$	$J_{11}(\omega x)$	$J_8^2(\omega x^2)$	$\cos(\sin(\omega x)+1)$	$\Gamma(0.5\cdot\sin(\omega x)+2)$
2^{40}	$[0, 500]$	5.4	5.7	7.2	7.3
2^{50}	$[0, 500]$	4.9	5.2	6.5	6.5
2^{60}	$[0, 500]$	4.5	4.7	6.0	5.9

QTT-ranks of M-vectors related to the function $I_{h_\omega,5}(\omega)$ sampled on a uniform grid in $[\omega_{\min}, \omega_{\max}]$.

QTT quadratures for highly oscillating d-dimensional integrals

$$I_{\mathcal{R}e}(\omega, L_{j_1,\dots,j_d}) = \int_{[-1,1]^d} L_{j_1}(y_1)\cdots L_{j_d}(y_d)\cos(\omega g(y))dy$$

Using a tensorized version of the Gauss-Legendre quadrature.

N	$[\omega_{\min}, \omega_{\max}]$	$g(x) = x_1 + x_2$	$g(x) = \sin(x_1)/\sqrt{x_1 x_2 + 3}$
2^{30}	$[0, 100]$	5.2	4.4
2^{40}	$[0, 100]$	4.6	3.9
2^{50}	$[0, 100]$	4.2	3.5

Table: **Effective QTT-ranks of N-vectors related to the function $I_{\mathcal{R}e}(\omega, L_{2,5})$ for $d = 2$ sampled on a uniform grid.**

N	$[\omega_{\min}, \omega_{\max}]$	$g(x) = x_1 + x_2 + x_3$	$g(x) = \sin(x_1 x_3)/\sqrt{x_1 x_2 + 3}$
2^{30}	$[0, 50]$	6.1	4.3
2^{40}	$[0, 50]$	5.5	3.9
2^{50}	$[0, 50]$	5.3	3.7

Table: **QTT-ranks of N-vectors related to the function $I_{\mathcal{R}e}(\omega, L_{2,5,3})$ for $d = 3$ sampled on a uniform grid.**

Periodic (geometric) homogenization for PDEs with oscillating features

[BNK, Repin '15]

Traditional FEM-Galerkin p.w.l. approximation in $\Omega = (0,1)^d$:

$$\textit{Find} \quad u_\epsilon \in H_0^1(\Omega): \quad -\operatorname{div}(a_\epsilon \nabla u_\epsilon) = f \quad \text{in } \Omega, \qquad f \in L^2(\Omega), \tag{1}$$

with **oscillating or lattice-structured/replicated** coefficients in $\Omega = \cup_i \Pi_{\mathbf{i}}^\epsilon$,

$$a_\epsilon(x) := \widehat{A}\left(\frac{x - x_i}{\epsilon}\right) \quad \text{in the scaled unit cell } \Pi_{\mathbf{i}}^\epsilon.$$

- Main computational problems: huge grids of size $\approx (n_0/\epsilon)^{-d}$, error control.

Example. $d = 3$, $n_0 = 100$, $\epsilon = 0.01$, then for $N \times N$ stiffness matrix, $N = 10^{12}$.

- Homogenization methods suggest asymptotically as $\epsilon \to 0$:

$$\|u_\epsilon - u_{homo}\| \le C\sqrt{\epsilon}.$$

Homogenization methods constructs the rough, strictly ϵ-dependent approximation in the case of perfect periodic coefficients, but "defected" boundary condit. (say, Dirichlet instead of periodic).

- In many applications the "defected" periodic coefficients arise (material science, lattice structured systems, uncertainty, etc.).

Examples of "defected" periodic coefficients: modulated functions

Principal questions:

– Defected periodic coefficients ?
– What if ϵ is not too small ?
– How to obtain the high precision independently of ϵ ?
– How to control the approximation error efficiently (adaptively) ?
– How to extend the homogenization approach to rather general class of (exotic) coefficients ?

Example.

$$a_\epsilon(x) = C + g(x)\sin(\omega x^m), \quad m = 1, 2, 3, ...$$

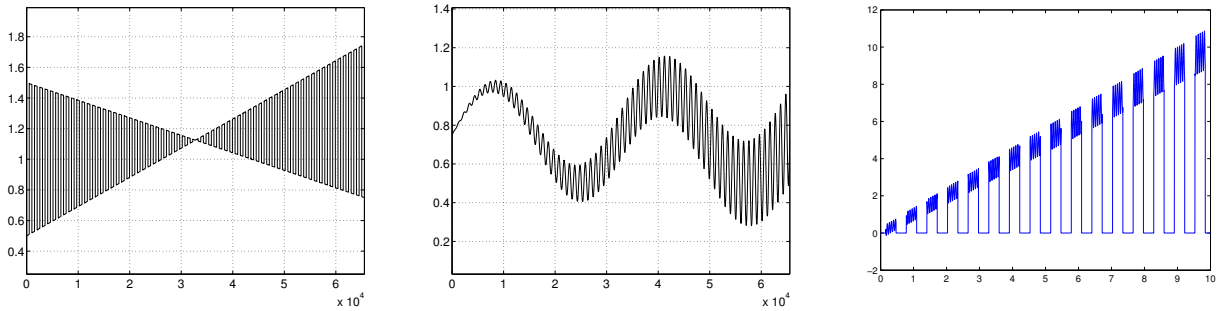

For all examples above the QTT ε-rank is of the order of $O(1)$ uniformly in the grid size !

QTT approximation of PDEs in periodic homogenization and beyond ...

Assume that (A) the solution of *homogenized approximation*, $a_0(x) = mean\{a_\epsilon(x)\} + C_0$,

$$\mathbb{A}_0\mathbf{u}_0 = \mathbf{f}, \tag{2}$$

is cheap and (B) for FEM-Galerkin approx. of (1), $\mathbb{A}_\epsilon$, the spectral equivalence holds

$$\lambda_0\mathbb{A}_0 \le \mathbb{A}_\epsilon \le \lambda_1\mathbb{A}_0, \quad \lambda_0, \lambda_1 > 0.$$

▶ **Basic idea** [BNK, Repin '15]. Solve the FEM-Galerkin approximation of (1)

$$\mathbb{A}_\epsilon\mathbf{u}_\epsilon = \mathbf{f}, \quad \mathbb{A}_\epsilon \in \mathbb{R}^{N^d\times N^d}, \quad \mathbf{u}_\epsilon, \mathbf{f} \in \mathbb{R}^{N^d}, \qquad N = 2^L \tag{3}$$

by rank-truncated preconditioned iteration in quantized tensor space $\mathbb{Q}_L$:

$$(\mathbb{E} + \beta\mathbb{A}_0^{-1}\mathbb{A}_\epsilon - \mathbb{E})\mathbf{u} \equiv (\mathbb{E} + \mathbb{B})\mathbf{u} = \beta\mathbf{u}_0, \quad \beta > 0,$$

assuming that for $\mathbb{B} = \beta\mathbb{A}_0^{-1}\mathbb{A}_\epsilon - \mathbb{E}$, $\|\mathbb{B}\| = q < 1$, and $rank_{QTT}(\mathbb{B})$ is small.

$$\text{Given } \mathbf{u}_0 \in \mathbb{Q}_L^{(r)}: \quad \mathbf{u}_{k+1} = \mathcal{T}_\varepsilon\left(\beta\mathbf{u}_0 - \mathbb{B}\mathbf{u}_k\right), \quad k = 0, 1, 2, ...$$

$$\|\mathbf{u}_{k+1} - \mathbf{u}_k\| \le q^k\|\mathbf{u}_0\|.$$

Lem. The condition number of the preconditioner $\mathbb{A}_0$ defined by $a_0(x)$ is bounded by

$$cond\{\mathbb{A}_0^{-1}\mathbb{A}_\epsilon\} \le C \max\frac{1+q(x)}{1-q(x)}, \quad \text{with} \quad q(x) := \frac{a^+(x) - a^-(x)}{a^+(x) + a^-(x)}.$$

Piece of theory: QTT-ranks of the 1D stiffness matrix on a fine grid

The stiffness matrix $A[a_\epsilon]$ reads

$$(A[a_\epsilon])_{i,i'} = (a_\epsilon(x)\nabla\varphi_i(x), \nabla\varphi_{i'}(x))_{L_2(\Omega)}, \quad i, i' = 1, \ldots, N,$$

$$A[a_\epsilon] = \frac{1}{h}\begin{bmatrix} a_1 + a_2 & -a_2 & & & \\ -a_2 & a_2 + a_3 & -a_3 & & \\ & \ddots & \ddots & \ddots & \\ & & -a_{N-1} & a_{N-1} + a_N & -a_N \\ & & & -a_N & 2a_N \end{bmatrix},$$

specified by the coefficient vector $\mathbf{a} = [a_i] \in \mathbb{R}^N$, $a_i = a_\epsilon(x_{i-1/2})$, $i = 1, \ldots, N$, $N = 2^L$.

Thm. [Dolgov, Kazeev, BNK, '13] Assume that the coefficient vector $\mathbf{a}$ is given in a QTT form

$$i \mapsto (j_1, ..., j_L) : \; a(i) = \sum_{\gamma_1, \ldots, \gamma_{L-1}=1}^{r_1, \ldots, r_{L-1}} a^{(1)}_{\gamma_1}(j_1) \cdots a^{(L)}_{\gamma_{L-1}}(j_L), \quad \text{with } r_p \le R, \; p = 1, \ldots, L-1.$$

Then

$$r_{QTT}(A[a_\epsilon]) \le 7R.$$

Proof: $A[a_\epsilon] = S\,\mathrm{diag}(\mathbf{a}) + \mathrm{diag}(\mathbf{a} + S\mathbf{a}) + \mathrm{diag}(\mathbf{a})S^\top$, where $S \in \mathbb{R}^{N\times N}$ means the upper shift matrix $S_{i,i'} = \begin{cases} 1, & i' = i+1, \\ 0, & \text{else}, \end{cases}$, for which we have $r_{QTT}(S) = 2$.

Recent contributions: [Kazeev, Oseledets, Rakhuba, Schwab '16]

Numerical examples for periodic and "defected" periodic coefficients: modulated functions

$$a_\epsilon(x) = C + g(x)\sin(\omega x^m), \quad m = 1, 2, 3, ..., \tag{4}$$

(left): $C = 1$, $g(x) = 1$, $m = 1$.
(middle): $C = 1$, $g(x) =$ step function, $m = 1$.
(right): $C = 1$, $g(x) = 1$, $m = 3$. $\omega = 2\,\pi\,32$, $\epsilon = \omega^{-1}$.

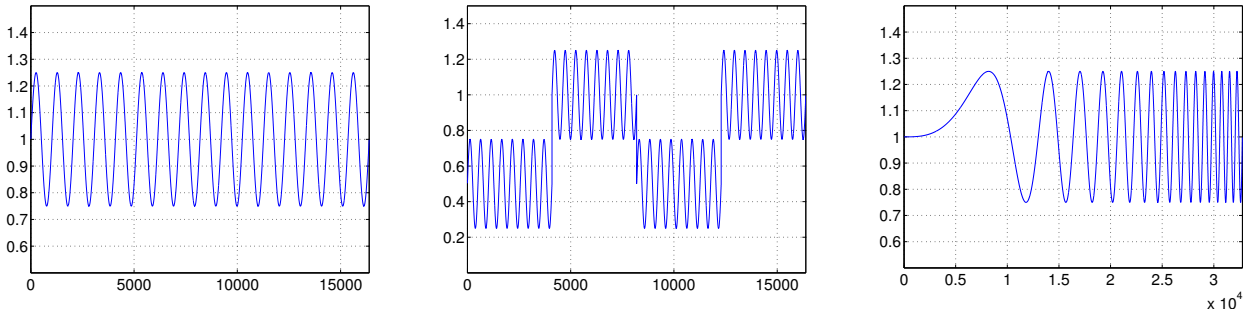

grid size 2^L	2^{13}, (it)	2^{14}, (it)	2^{15}, (it)	2^{16}, (it)	2^{17}, (it)	$r(\mathbf{a}_\epsilon)$	$r(\mathbf{u}_\epsilon)$
$C + \sin(\omega x)$	0.97, (5)	1.2, (5)	1.3, (5)	2.0, (6)	2.1, (6)	2.67	3.7
4-steps coef.	3.4, (9)	4.3, (9)	4.5, (9)	6.7, (9)	14.3, (14)	2.9	4.96
$C + \sin(\omega x^3)$	5.3, (5)	10.0, (6)	9.95, (6)	11.98, (6)	16.2, (5)	7.53	8.24

CPU sec., iter. history, QTT-ranks with $\omega = 1/\epsilon = 2\pi 64$, $\varepsilon_{QTT} = 10^{-7}$: $\|u_\epsilon - \mathbf{u}_\epsilon\|_1 \backsimeq 10^{-5} - 10^{-6}$.

QTT rank-truncated iter. of logarithmic cost, $O(\log N)$, vs. homogenization method

[BNK, Repin '14-'15].
– Uniform convergence rate of preconditioned iteration,
– approximation of order $O(h^2)$ uniformly in ϵ,
– logarithmic complexity of order $O(\log n) = O(\log \frac{1}{\epsilon})$.

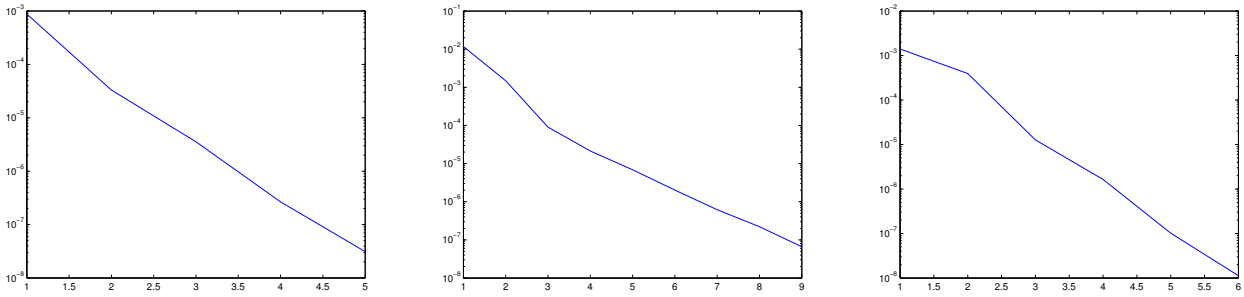

Precond. Steepest Descent in QTT-truncated iterations for the periodic, step-, and cubically-oscillating coef.

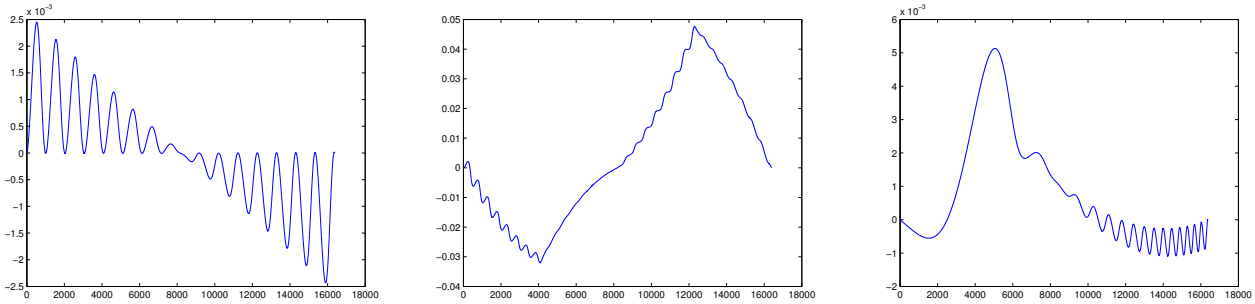

Difference between exact and homogenized solutions (no convergence in gradients !).

Low-rank reduction in homogenization: $O(1/\epsilon^d) \to O(d/\epsilon) \to O(d|\log\epsilon|)$

Quasi-periodic coefficients $a_\epsilon(x) > 0$, $d \geq 1$,

$$\mathcal{A}u_\epsilon := -\mathrm{div}(a_\epsilon(x)\mathrm{grad}\, u_\epsilon) = f(x), \quad x \in \Omega = (0,1)^d, \quad u_{\epsilon|\partial\Omega} = 0, \tag{5}$$

$f(x_1,\dots,x_d)$ and $a_\epsilon(x)$ can be approximated with the low separation rank.

- Apply the Galerkin discretization of eqn. (5) by means of tensor-product pwl FEM

$$\{\varphi_i(x) := \varphi_{i_1}(x_1)\cdots\varphi_{i_d}(x_d)\}, \quad i = (i_1,\dots,i_d), \quad i_\ell \in \{1,\dots,n_\ell\},\ \ell = 1,\dots,d.$$

- The univariate grid size $n_\ell = O(1/\epsilon) \Rightarrow$ the total problem size $N = O(1/\epsilon^d)$.

- $d = 2$, $a(x_1,x_2) = \sum_{k=1}^{R} a_k^{(1)}(x_1)a_k^{(2)}(x_2) > 0$. For $R = 1$: $a(x_1,x_2) = a^{(1)}(x_1)a^{(2)}(x_2)$.

Example of a periodic oscillating coefficient (left) and the respective 1D factor, $a^{(1)}(\cdot)$.

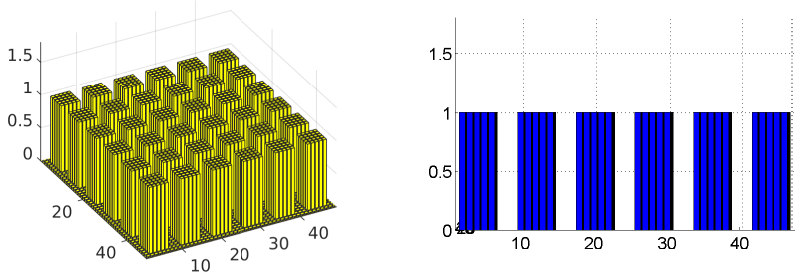

Asymptotic homogenization: Galerkin matrix in Kronecker product form

- For the entries of the Galerkin stiffness matrix $A = [a_{ij}] \in \mathbb{R}^{N\times N}$:

$$\begin{aligned} a_{ij} &= \langle \mathcal{A}\varphi_{\mathbf{i}}, \varphi_{\mathbf{j}} \rangle = \int_{\Omega} a^{(1)}(x_1)a^{(2)}(x_2)\nabla\varphi_i \cdot \nabla\varphi_j dx \\ &= \int_{(0.1)} a^{(1)}(x_1)\frac{\partial\varphi_{i_1}(x_1)}{\partial x_1}\frac{\partial\varphi_{j_1}(x_1)}{\partial x_1}dx_1 \int_{(0.1)} a^{(2)}(x_2)\varphi_{i_2}(x_2)\varphi_{j_2}(x_2)dx_2 \\ &+ \int_{(0.1)} a^{(1)}(x_1)\varphi_{i_1}(x_1)\varphi_{j_1}(x_1)dx_1 \int_{(0.1)} a^{(2)}(x_2)\frac{\partial\varphi_{i_2}(x_2)}{\partial x_2}\frac{\partial\varphi_{j_2}(x_2)}{\partial x_2}dx_2, \end{aligned} \tag{6}$$

$$A = [a_{ij}] = A_1 \otimes M_2 + M_1 \otimes A_2.$$

$A_1 = [a_{i_1 j_1}] \in \mathbb{R}^{n_1\times n_1}$ and $A_2 = [a_{i_2 j_2}] \in \mathbb{R}^{n_2\times n_2}$ – the univariate stiffness matrices,
$M_1 = [m_{i_1 j_1}] \in \mathbb{R}^{n_1\times n_1}$ and $M_2 = [m_{i_2 j_2}] \in \mathbb{R}^{n_2\times n_2}$ – the weighted mass matrices,

$$a_{i_1 j_1} = \int_{(0.1)} a^{(1)}(x_1)\frac{\partial\varphi_{i_1}(x_1)}{\partial x_1}\frac{\partial\varphi_{j_1}(x_1)}{\partial x_1}dx_1, \quad m_{i_1 j_1} = \int_{(0.1)} a^{(1)}(x_1)\varphi_{i_1}(x_1)\varphi_{j_1}(x_1)dx_1.$$

- By lamping of the mass matrices

$$A \mapsto A = A_1 \otimes I_2 + I_1 \otimes A_2.$$

Asymptotic homogenization: rank analysis

$R = 1 \Rightarrow$ a prototype preconditioner for solving the linear system for $R > 1$

$$A\mathbf{u} = \mathbf{f} \quad \text{with} \quad \mathbf{f} = \sum_{k=1}^{R_f} \mathbf{f}_k^{(1)} \otimes \mathbf{f}_k^{(2)}, \quad \mathbf{f}_k^{(\ell)} \in \mathbb{R}^{n_\ell}. \tag{7}$$

In the general case $d \geq 2$ and $R \geq 1$: $\mathrm{rank}_{Kron}(A) = d\,R$.
- The existence of the low rank solution to the eqn. (7) by the sinc-quadrature approx. to the Laplace transform [Gavrilyuk, Hackbusch, BNK '05]

$$A^{-1} = \int_{\mathbb{R}_+} e^{-tA}dt \approx B_M := \sum_{k=-M}^{M} c_k e^{-t_k A} = \sum_{k=-M}^{M} c_k e^{-t_k A_1} \otimes e^{-t_k A_2}.$$

Hint for proof: the matrices A_1 and A_2 commute with I_1 and I_2, respectively.

$$\|A^{-1} - B_M\| \leq Ce^{-cR_A}\|A^{-1}\|, \quad R_A = (2M+1) = O(|\log\epsilon|).$$

$$\mathbf{u} = A^{-1}\mathbf{f} \approx \sum_{k=-M}^{M} c_k \sum_{m=1}^{R_f} e^{-t_k A_1}\mathbf{f}_m^{(1)} \otimes e^{-t_k A_2}\mathbf{f}_m^{(2)}.$$

Asymptotic homogenization: rank analysis of the solution

The rank behavior in the SVD decomposition of the solution in the case of 8×8 periodic coefficient [BNK, Repin '16].

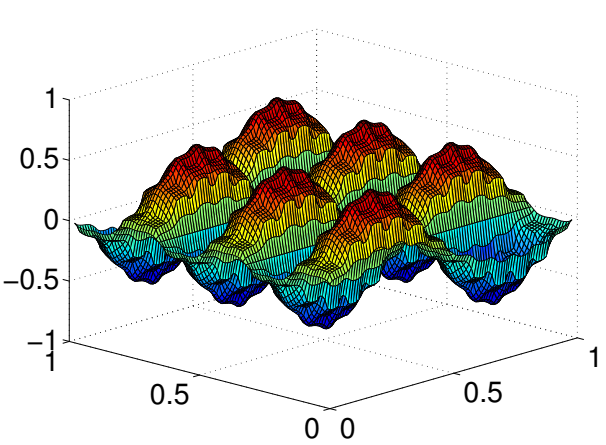

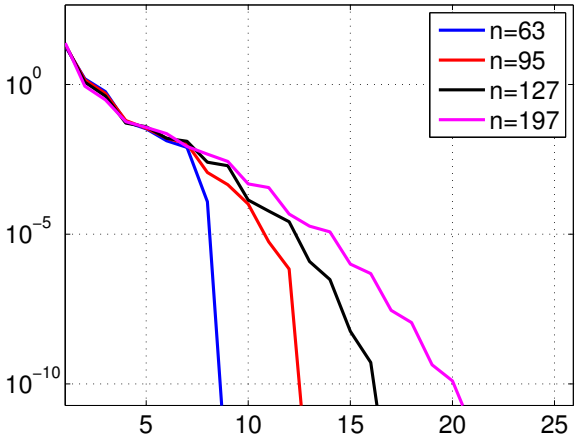

▶ The exponential decay of the approximation error in the rank parameter does not depend on the $L \times L$ lattice size in the coef., i.e. on $\epsilon = 1/L$.

From geometric to stochastic homogenization ...

▶ Solution on 400×400-grid, $f_1(x_1, x_2) = \sin(2\pi x_1)\sin(2\pi x_2)$. [BNK, Repin '16].
The PCG solver for eqn. (7) demonstrates robust convergence rate $q \ll 1$ (6 iter. for $\delta = 10^{-6}$).

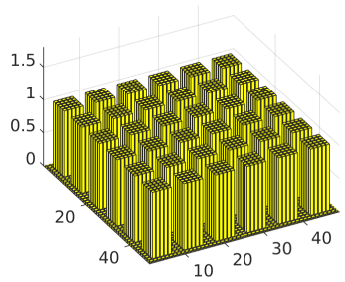

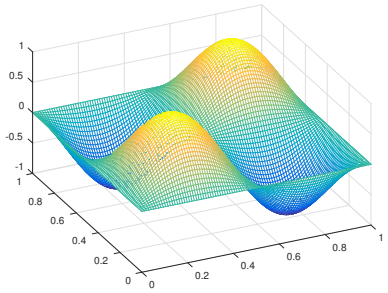

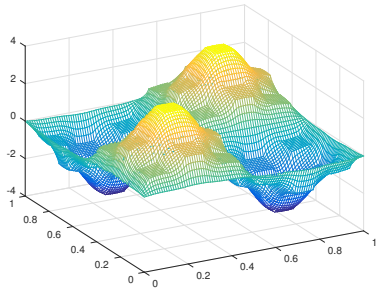

Towards stochastic homogenization

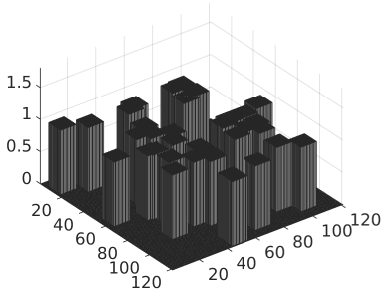

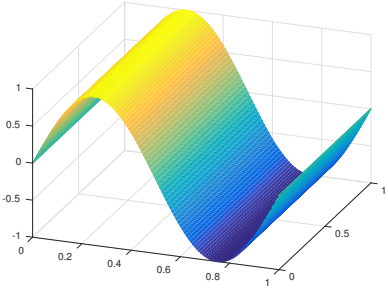

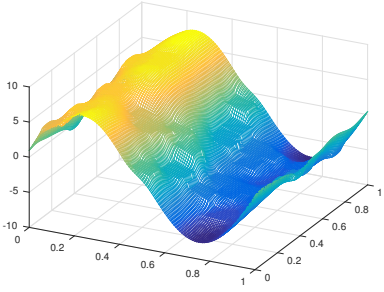

Iso-Geometric Analysis (IGA): Matrix generation via low-rank approx.

[Mantzaflaris, Jüttler, BNK, Langer: '15 - '16]

▶ **Low-rank IGA in 2D and 3D: elliptic PDEs on complicated geometry**.

FEM-Galerkin approximation in $\Omega \in \mathbb{R}^d$ by a patch-wise mapping onto reference domain:

$$\textit{Find} \quad u \in H_0^1(\Omega): \quad -\operatorname{div}(a(x)\nabla u) = f \quad \text{in } \Omega, \quad f \in L^2(\Omega).$$

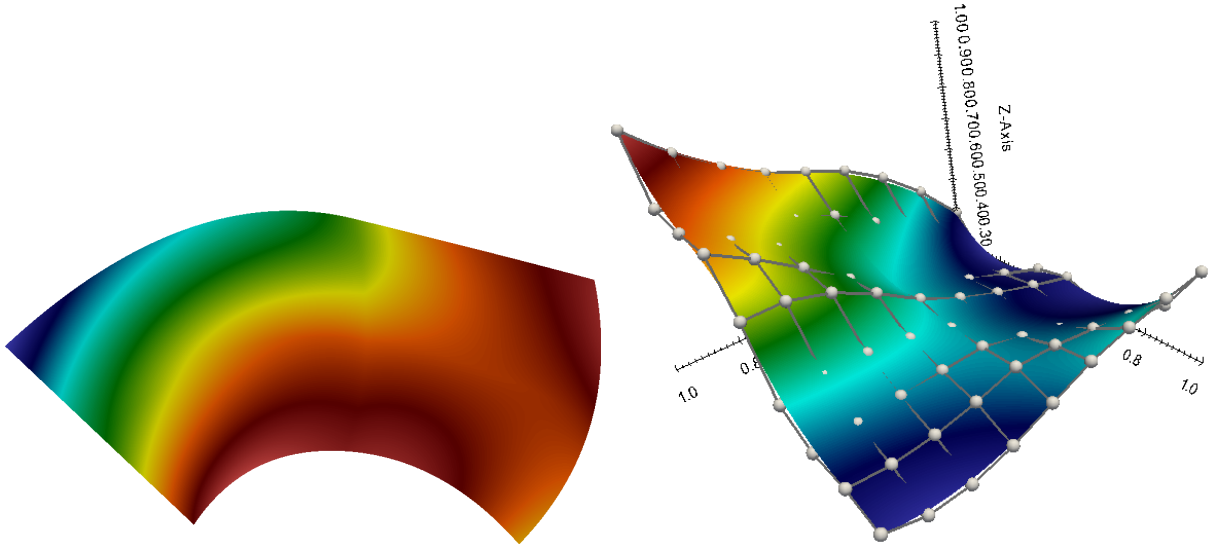

Figure: **The Jacobian determinant values of the selected patch (Fig. 2) on the domain (left). The graph and control net in parameter domain (right).**

IGA: Multi-patch low-rank representation

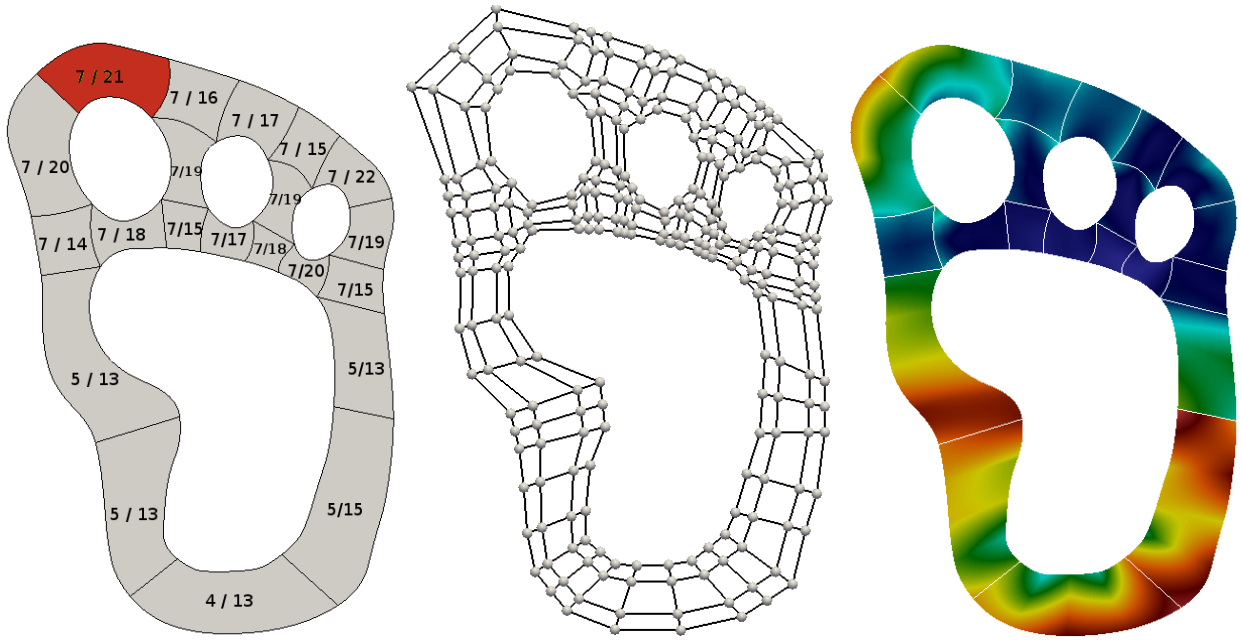

Figure: **The yeti footprint domain, parameterized by 21 quadratic B-spline patches. Patch segmentation (left), control grids (middle) and the (absolute) Jacobian determinant are shown. On the left picture rank(det ∇G) and max(rank($q_{k,\ell}$), $k, \ell \in \{1, 2\}$) are given. $\epsilon = 10^{-10}$.**

The canonical (CP) tensor approximation of the Newton kernel $\frac{1}{\|x\|}$

[Braess '95], [Stenger '93], [Gavrilyuk, Hackbusch, BNK '05], [Bertoglio, BNK '08]

$$\mathbf{P} := [p_{\mathbf{i}}] \in \mathbb{R}^{n\times n\times n}, \quad p_{\mathbf{i}} = \int_{\mathbb{R}^3} \frac{\psi_{\mathbf{i}}(\mathbf{x})}{\|\mathbf{x}\|}\mathrm{d}\mathbf{x}, \quad \psi_{\mathbf{i}}(\mathbf{x}) = \prod_{\ell=1}^{d} \psi_{i_\ell}^{(\ell)}(x_\ell),\ \{i_\ell\}_1^{n_\ell},\ \ell = 1,\,2,\,3.$$

Use the Laplace-Gauss transform for the analytic function $p(z) = \frac{1}{z} = \frac{1}{\|x\|} = \frac{1}{\sqrt{x_1^2+x_2^2+x_3^2}}$,

$$\frac{1}{z} = \frac{2}{\sqrt{\pi}} \int_{\mathbb{R}_+} e^{-t^2 z^2} dt \approx \sum_{k=-M}^{M} a_k e^{-t_k^2 \|x\|^2} = \sum_{k=-M}^{M} a_k \prod_{\ell=1}^{3} e^{-t_k^2 x_\ell^2}.$$

$0 < h \le \|x\| \le A < \infty$: sinc-quadrature approximation converges exponentially in M:

$$\left| \frac{1}{\|x\|} - \sum_{k=-M}^{M} a_k e^{-t_k^2\|x\|^2} \right| \le \frac{C}{a}\, e^{-\beta\sqrt{M}}, \quad \text{with some } C, \beta > 0,$$

where the quadrature points and weights are given by ($a(t_k) = \frac{2}{\sqrt{\pi}}$)

$$t_k = k\hbar_M, \quad a_k = a(t_k)\hbar_M, \quad \hbar_M = C_0 \log(M)/M, \quad C_0 > 0.$$

Application to a general class of radial basis functions, Green's kernels

RS-tensor approximation applies to a wide class of long-range RB funct. $p(\|x\|)$ in $\mathbb{R}^3$:

Slater function: $p(\|x\|) = \exp(-\lambda\|x\|), \quad \lambda > 0,$

Yukawa kernel: $p(\|x\|) = \dfrac{\exp(-\lambda\|x\|)}{\|x\|}, \quad \lambda > 0,$

Lennard-Jones potential: $p(\|x\|) = 4\epsilon \left[\left(\dfrac{\sigma}{\|x\|}\right)^{12} - \left(\dfrac{\sigma}{\|x\|}\right)^{6} \right],$

The simplified version of the Lennard-Jones potential, the Buckingham function

Buckingham potential: $p(\|x\|) = 4\epsilon \left[e^{\|x\|/r_0} - \left(\dfrac{\sigma}{\|x\|}\right)^{6} \right].$

The electrostatic dipole-dipole potential energy (Van der Waals forces)

Dipole-dipole interaction energy: $p(\|x\|) = \dfrac{C_0}{\|x\|^3}.$

CP tensor approx. of the single Newton kernel $p(\|x\|) = \frac{1}{\|x\|}$ on fine grid

$$\mathbf{P} \approx \mathbf{P}_R = \sum_{k=-M}^{M} a_k \bigotimes_{\ell=1}^{3} \mathbf{b}^{(\ell)}(t_k) = \sum_{q=1}^{R} \mathbf{p}_q^{(1)} \otimes \mathbf{p}_q^{(2)} \otimes \mathbf{p}_q^{(3)} \in \mathbb{R}^{n\times n\times n}, \quad R \le 2M+1 \approx C|\log\varepsilon|.$$

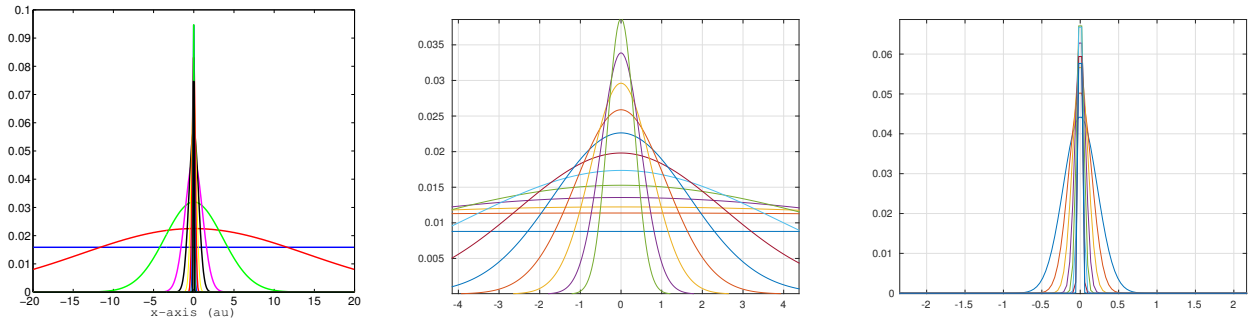

grid size n^3	8192^3	16384^3	32768^3	65536^3	131072^3
Time (s)	6	16	61	241	1000
Canonical rank R	34	37	39	41	43
Compression rate	$2\cdot 10^6$	$7\cdot 10^6$	$2\cdot 10^7$	$1\cdot 10^8$	$4\cdot 10^8$

CPU times (Matlab) to compute canonical tensor $\mathbf{P}_R$, tol. $\varepsilon = 10^{-7}$.

Range-separated (RS) tensor format for approximating funct. with multiple cusps

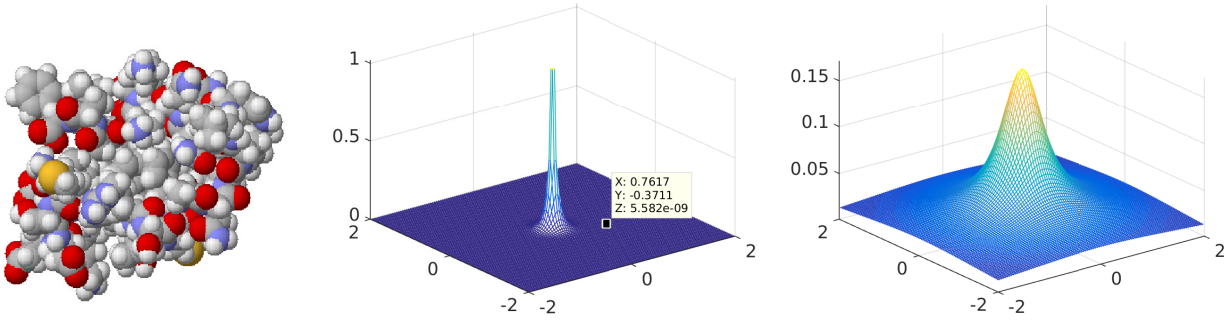

Figure: *Villin protein (left). Short- and long-range parts of the reference Newton kernel* $1/\|x\|$.

[Benner, Khoromskaia, BNK '16]

Definition

(RS-canonical tensors). The RS-canonical tensor format defines the class of d-tensors $\mathbf{A} \in \mathbb{R}^{n_1\times\cdots\times n_d}$, represented as a sum of a rank-R CP tensor $\mathbf{U}$ and a cumulated CP tensor generated by localized $\mathbf{U}_0$, s.t. $\mathrm{rank}(\mathbf{U}_\nu) = \mathrm{rank}(\mathbf{U}_0) \le R_0$, $\mathbf{U}_\nu = \mathrm{Replica}(\mathbf{U}_0)$,

$$\mathbf{A} = \sum_{k=1}^{R} \xi_k \mathbf{u}_k^{(1)} \otimes \cdots \otimes \mathbf{u}_k^{(d)} + \sum_{\nu=1}^{N_0} c_\nu \mathbf{U}_\nu, \quad \text{with} \quad \mathrm{diam}(\mathrm{supp}\mathbf{U}_\nu) \le 2\gamma.$$

RS canonical format: beneficial properties

▶ RS-canonical tensor $\mathbf{A} \in \mathbb{R}^{n_1 \times \cdots \times n_d}$ is uniquely defined by the following parametrization: rank-R CP tensor $\mathbf{U}$, the rank-R_0 reference CP tensor $\mathbf{U}_0$ with mode-size bounded by 2γ, list $\mathcal{J}$ of the coordinates and weights of N_0 particles in $\mathbb{R}^d$.

Theorem

[Benner, Khoromskaia, BNK '16] *The storage size for RS-canonical tensor is estimated by*

$$stor(\mathbf{A}) \leq dRn + (d+1)N_0 + dR_0\gamma.$$

Each entry of an RS-CP tensor can be calculated at $O(dR + 2d\gamma R_0)$ cost.
ε-rank $\mathbf{r}_0$ of the Tucker approximation to the long-range CP tensor $\mathbf{U}$ is bounded by

$$|\mathbf{r}_0| := rank_{Tuck}(\mathbf{U}) \leq C\, b\, \log^{3/2}(|\log(\varepsilon/N_0)|).$$

Lemma

The following operations on RS canonical/Tucker tensors can be realized efficiently:
(a) construction of functional interpolants in $\mathbb{R}^d$ via radial basis functions.
(b) summation of many-particle interaction potentials meshed up on a fine grid in $\mathbb{R}^d$.
(c) computation of interaction energy, gradients and forces for many-particle system.

Bounds on tensor rank in Theorem: analysis in the frequency domain

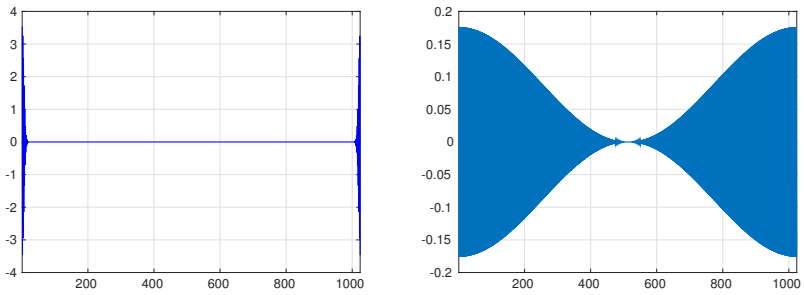

Figure: *Fourier coef. of the long- (left) and short-range (right) discrete Gaussians, $n = 1024$.*

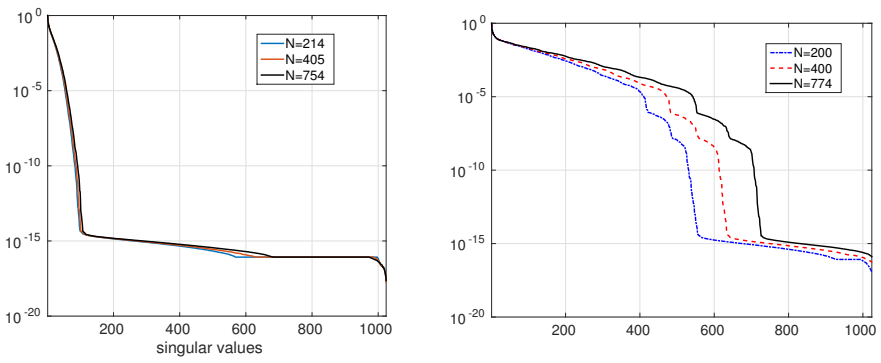

Figure: *Mode-1 singular values of side matrices for the full sum and long-range part P_l vs. N_0, $R_l = 12$.*

RS canonical format: how to split short and long range parts

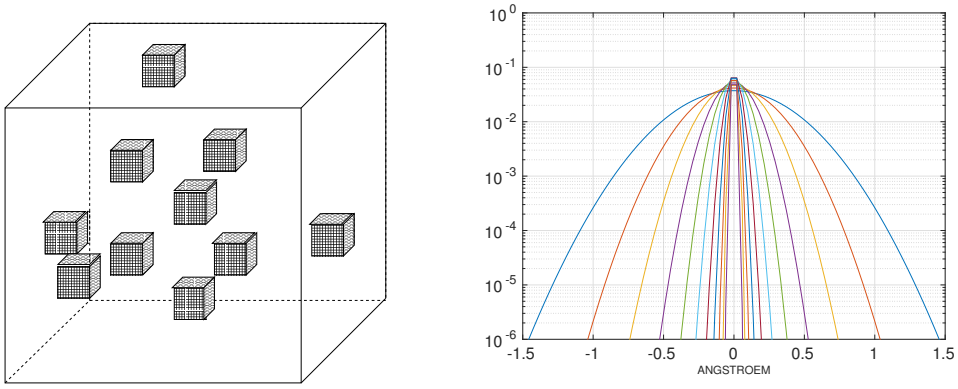

Figure: *Effective supports of the CCT (left); short-range canonical vectors for* $k = 1, \ldots, 11$ *on log-scale.*

- The classes of RS-Tucker and RS-TT tensors are defined completely similar.

N_0 / R_l	8	9	10	11	12	13
200	10,10,11	13,12,12	18,15,16	23,19,21	32,24,27	42,30,34
400	11,10,11	14,13,14	19,16,20	26,21,26	35,27,36	47,34,47
782	11,11,12	15,14,15	20,18,20	28,26,27	39,35,37	52,46,50

Table: *Tucker ranks* $\mathbf{r} = (r_1, r_2, r_3)$ *for the long-range part of* N_0*-nuclei electrostatic potential in a protein,* $\epsilon = 10^{-6}$.

Initial applications of RS-tensors: Multi-dimensional data modeling

- **Scattered data modeling:** the approximation of multi-variate func. $f : \mathbb{R}^d \to \mathbb{R}$ by sampling at a finite set $\mathcal{X} = \{x_1, \ldots, x_N\} \subset \mathbb{R}^d$ of p.w. distinct points.

For f: the surface of a solid body, the solution of a PDE, many-body potential field, etc.

- Traditional ways of recovering f from a sampling vect. $f_{|\mathcal{X}} = (f(x_1), \ldots, f(x_N))$: constructing a functional interpolant $P_N : \mathbb{R}^d \to \mathbb{R}$ s.t. $P_{N|\mathcal{X}} = f_{|\mathcal{X}} =: \mathbf{f} \in \mathbb{R}^N$, i.e.,

$$P_N(x_j) = f(x_j), \quad \forall\, 1 \le j \le N. \tag{8}$$

Using *radial basis (RB) functions*: find interpolants P_N in the form

$$P_N(x) = \sum_{j=1}^{N} c_j p(\|x - x_j\|) + Q(x), \quad Q \text{ is some smooth function, say } Q = 0, \tag{9}$$

$p = p(r) : [0, \infty) \to \mathbb{R}$ is a fixed RB function, $r = \|\cdot\|$ is the Euclidean norm on $\mathbb{R}^d$.

Examples: $p = r^\nu$, $(1 + r^2)^\nu$, $(\nu \in \mathbb{R})$, $\exp(-r^2)$, $r^2 \log(r)$.

[Buhmann, 2003]

RS tensor approach to multi-dimensional data modeling: general overview

[Benner, Khoromskaia, BNK '16]

(A) Fixed coefficient vector $\mathbf{c} = (c_1, \ldots, c_N)^T \in \mathbb{R}^N$:
efficiently representing the interpolant $P_N(x)$ on fine tensor grid in $\mathbb{R}^d$ s.t.
(a) $O(1)$-fast point evaluation of P_N in the computational volume Ω,
(b) computation of various integral-differential operations on that interpolant
(gradients, forces, scalar products, convolution integrals, etc.).

(B) Finding the coefficient vector $\mathbf{c}$ that solves the interpolation problem (8).

- Problem (A) exactly fits our RS tensor framework !
- Problem (B): Use favorable iteration for solving coeff. vector $\mathbf{c} = (c_1, \ldots, c_N)^T$,

$$A_{p,\mathcal{X}}\mathbf{c} = \mathbf{f}, \quad \text{with} \quad A_{p,\mathcal{X}} = A_{p,\mathcal{X}}^T = [p(\|x_i - x_j\|)]_{1\le i,j\le N} \in \mathbb{R}^{N\times N}. \tag{10}$$

Assume $\mathcal{X} = \Omega_h$ be the $n^{\otimes d}$-set of grid-points, i.e., $N = n^d$.
The d-tuple multi-index $\mathbf{i} = (i_1, \ldots, i_d)$, $\mathbf{j} = (j_1, \ldots, j_d)$: reshape $A_{p,\mathcal{X}}$ into the tensor

$$A_{p,\mathcal{X}} \mapsto \mathbf{A} = [a(i_1, j_1, \ldots, i_d, j_d)] \in \bigotimes_{\ell=1}^{d} \mathbb{R}^{n\times n}, \quad \mathbf{A} = \mathbf{A}_{R_s} + \mathbf{A}_{R_l}.$$

$\mathbf{A}_{R_s}$ - diagonal, $\mathbf{A}_{R_l} = \sum_{k=1}^{R_l} A_k^{(1)} \otimes \cdots \otimes A_k^{(d)}$ $\Rightarrow$ **Storage:** $O(N + dR_l n)$, MVP is simple.

The Poisson-Boltzmann eqn. for electrostatic potential of a protein

The linearized Poisson-Boltzmann (PB) equation [Holst et al. '08]

$$-\nabla\cdot(\epsilon\nabla u) + \kappa^2 u = \rho_f = \sum_{k=1}^{N} z_k \delta(\|x - x_k\|) \quad \text{in} \quad \Omega, \tag{11}$$

where u is the target electrostatic potential of a protein, ρ_f is the scaled singular charge distribution supported at points $x_k \in \Omega_m$, $\kappa = 0, \epsilon = 1$ in Ω_m.
The interface conditions on the interior boundary $\Gamma = \partial\Omega_m$: $[u] = 0$, $\left[\epsilon \frac{\partial u}{\partial n}\right]$ on Γ.

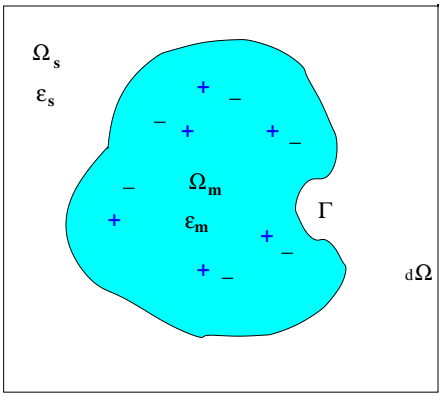

Figure: **Computational domain for PBE: Solute (molecule) region Ω_m, solvent Ω_s.**

Reduced basis method for PBE: [Kweyu, Hess, Feng, Stein, Benner: '16]

New regularization scheme for the PB eqn.: the RS-tensor approach

The additive splitting in Ω: $u = u^r + u^\rho$ s.t. $u^\rho = 0$ in Ω_s.

$$\text{For singular component:} \quad -\epsilon_m \Delta u^\rho = \rho_f \quad \text{in} \quad \Omega_m; \quad u^\rho = 0 \quad \text{on} \quad \Gamma. \qquad (12)$$

Facilitate solving of (12): use the free space singular potential in form of RS tensor

$$P_0(x) = \sum_{k=1}^{N} z_k / \|x - x_k\| : \quad \epsilon_m \Delta P_0 = \rho_f \quad \text{in} \quad \mathbb{R}^3,$$

let $P^s = P_{0|\overline{\Omega}_m}$ in $\overline{\Omega}_m$; $\quad P^s = 0$ in Ω_s, and set $u^\rho = P^s + u^h$.
A harmonic function u^h compensates the discontinuity of P^s on Γ,

$$\Delta u^h = 0 \quad \text{in} \quad \Omega_m; \quad u^h = -P^s \quad \text{on} \quad \Gamma.$$

- [Benner, Khoromskaia, BNK '16] Eqn. (11) is transformed to that for the regular potential u^r:

$$-\nabla \cdot (\epsilon \nabla u^r) + \kappa^2 u^r = 0 \quad \text{in} \quad \Omega,$$

$$[u^r] = 0, \quad \left[\epsilon \frac{\partial u^r}{\partial n}\right] = -\epsilon_m \frac{\partial u^\rho}{\partial n}, \quad \text{on} \quad \Gamma.$$

- Benefit: $\partial_n u^\rho{}_{|\Gamma}$ depends only on the long-range part in $P_0(x) \Rightarrow$ low-rank tensor.

Conclusions

Fast tensor numerical methods for multi-dimensional PDEs

- Efficient multi-linear algebra of formatted tensors in CP, Tucker, TT formats (+).
- Advanced $O(d \log N)$ tensor formats: QCan, QTT, QTT-Tucker (+).
- "Canonical" convolution of $N^{\otimes d}$ tensors in $O(dN)$ op. (+).
- Grid-based tensor factorization of the two-electron integrals (+).
- Tensor solver for the Hartree-Fock equation (+).
- Fast lattice summation of long-range potentials and the novel RS tensor format.
- Fast integration of highly oscillating functions and efficient solvers for PDEs with oscillating coefficients (±).
- The Fokker-Planck and master equations (±).
- Stochastic/parametric PDEs (±).

Novel super-fast data transforms of logarithmic cost:

- QTT convolution(d) in $O(d \log N)$ operations (±).
- Super-fast QTT-FFT(d) (competing to sparse and quantum FFT) (+).
- Fast wavelet transform in quantized space with logarithmic cost (±).

Thank you very much for your interest !